Control Engineering Practice 47 (2016) 48–59

Contents lists available at ScienceDirect

Control Engineering Practice

journal homepage: www.elsevier.com/locate/conengprac

Parametric sensitivity and control of on-orbit manipulators during impacts using the Centre of Percussion concept

Iosif S. Paraskevas, Evangelos G. Papadopoulos *

School of Mechanical Engineering, National Technical University of Athens (NTUA), 9 Heroon Polytechneiou Street, 15780 Athens, Greece

ARTICLE INFO

Article history:
Received 30 May 2014
Received in revised form
23 October 2015
Accepted 11 December 2015

Keywords:
Space robots
Centre of percussion
Control method during impacts
Impact reactions compensation

ABSTRACT

During capture of a free-flying object, a robotic servicer can be subject to impacts, which may separate it from the object or damage crucial subsystems. However, the reactions can be minimized using the Centre of Percussion (CoP) concept. Following a brief introduction of the two- and three-dimensional cases, the performance of a robot under impact is assessed when the CoP concept is employed. The effects of the parametric uncertainties on manipulator joint reactions are studied. A control method to compensate for the reaction forces is proposed. Implementation guidelines are discussed. Simulations of a planar space robot validate the analysis.

1. Introduction

Space exploration and exploitation require robust human and robotic infrastructure on orbit and beyond. To this end, tasks like satellite servicing, orbital debris removal and construction of large assemblies on Earth or other planetary orbits will be of critical importance in the near future. Since On-Orbit Servicing (OOS) plays a central role to the future of space programmes, space agencies have already incorporated OOS activities in their roadmaps, with notable examples the ETS-VII from JAXA, the Orbital Express and the Robotic Refuelling Mission (RRM) from NASA, as well as a number of research activities in the Clean Space initiative and the Automation and Robotics group of ESA.

To perform a robotic servicing mission, it is necessary to reach and grab a target (satellite or debris). Assuming a space robot already on orbit, this procedure includes the phases of far and close rendezvous, of mating (docking or berthing which incorporate capture of some kind), and of servicing (Fehse, 2008). The capture of a target by a space robotic system, consisting of a satellite base and of one or more manipulators mounted on it, is a demanding task. The dynamic coupling between the base and the manipulator complicate system analysis and control (Papadopoulos & Moosavian, 1994). During capture, impact forces appear, as the chaser and the target come into contact. This task becomes more challenging when the robotic system and the target have comparable masses. To minimize reaction forces, the reduction of body impulses using the Extended Inertia Tensor has been proposed (Yoshida & Sashida, 1993), and the concepts of virtual mass and impedance matching of systems were studied (Yoshida & Nakanishi, 2003). Related research works focus on the problem taking into account the system dynamics and the post-impact behaviour (Dimitrov & Yoshida, 2004), or the condition prior to impact, e.g. by incorporating an optimal approach method (Flores-Abad, Pham, & Ma, 2012).

In this work, a method for minimizing undesired reaction forces during impacts is presented, which exploits the physical characteristics of bodies rotating about an axis. The method is based on the notion of the Centre of Percussion (CoP) or Percussion Point. Its primary use is in sports equipment (e.g. tennis rackets, baseball bats) and hand tools (e.g. hammers). For example, if an external force acts on a bat's CoP, less stress is produced at the hands of a player (sweet spot) (Cross, 2004). The CoP has been of limited use so far in other areas although some interesting works appeared recently. A novel method, which exploits the CoP for legged locomotion is proposed, by considering the foot while in stance, as a pivot (Alba et al., 2010) Another work for bipeds studies the CoP in weight lifting (Arisumi et al., 2007). The use of CoP to minimize the reactions on a wagon when it encounters an object has been proposed (Ioi et al., 2011). The existence of multiple CoPs at flexible beams was also presented (Svinin, Kaneko, and Yamamoto, 2011). Generally, the analytical treatment in the bibliography is scarce. However the CoP can be exploited further in space applications (Papadopoulos & Paraskevas, 2005; Paraskevas & Papadopoulos, 2013).

In general, any reduction of the reaction forces on robot joint bearings is welcome, as it reduces the developed stresses and

* Corresponding author.
E-mail addresses: isparas@mail.ntua.gr (I.S. Paraskevas), egpapado@central.ntua.gr (E.G. Papadopoulos).

http://dx.doi.org/10.1016/j.conengprac.2015.12.004
0967-0661/

consequently the probability of a mechanical failure. Additionally, and especially for space systems, any reduction in reactions minimizes the translational forces that affect the free-flyer base, minimizing the tendency of the chaser to move away from the target after an impact; this is particularly important in the event of an unsuccessful capture. Staying close to the target also minimizes the fuel that would be required to approach the target again. To this end the interesting property of CoP to theoretically cancel out reaction forces seems beneficial for a robot interacting with its environment. However it is necessary to examine its performance in three-dimensional tasks and thoroughly examine its sensitivity to system parameters. As impacts are by nature processes with fast dynamics, it is important to estimate how such sensitivity may affect performance both during the design phases, and during its field tasks.

The CoP is a property associated usually with free rotating joints. This is true also in robotics, and requires a passive joint – for example by disengaging the motors of a joint before the impact. However either this is not always possible, or the joint bearings cannot be considered as perfectly frictionless. Robotic systems on orbit have rotational joints and usually use Harmonic Drives (HD), which are rigidly connected to the links (Hauschild & Heppler, 2007) Disregarding the backlash (zero for HDs), gear friction is a problem present on all kinds of transmission systems (Li & Mao, 2013). Additionally, it is not always possible to have a perfect impact at a particular point – thus a compensation measure must be implemented to reduce the reaction forces. Confronting these issues resembles the approaches taken in rehabilitation robotics. Indeed in such robots, it is necessary for patients with reduced neural or muscular capabilities to move links according to the prescribed therapy. In those cases even small frictional torques are undesired (Kong et al., 2009). Here, a similar approach is considered, using the concept presented in the work of Nef and Lum (2009). For this reason, a controller, which exploits the CoP is proposed. In the literature, the CoP has been used mainly as a reference point, while a number of controllers (e.g. PD) are used to set the motor torques (Alba et al., 2010; Arisumi et al., 2007). To the best of the authors' knowledge, this is the first time that the CoP is used in the core calculation of control torques.

This paper establishes in Section 2 the theoretical basis for the CoP, for the planar and the three-dimensional cases, and introduces the notion of the Coefficient of Impact Design. In Section 3, the effects of uncertainties on system or impact parameters are examined using non-dimensional variables, allowing task performance assessment. In Section 4, the theory of the CoP is established for multibody systems using the Newton–Euler Approach (NEA). Its use in robotic systems is presented, and a control method exploiting the concept at non-free joints is developed. Implementation guidelines for various manipulator types are discussed in Section 5. Finally in Section 6, simulation results for a planar space robot system confirm the benefit of using the CoP during tasks that include impacts.

2. Generalised theory of Centre of Percussion

In this section, a concise theoretical analysis of the CoP in 2D and 3D is presented as a prerequisite in developing the parametric analysis and the associated controller. The assumptions made here are outlined, next.

2.1. Assumptions

The following assumptions apply:

(1) Impacts occur between rigid bodies. The contact area remains small in comparison to other body dimensions. Body flexibilities are not considered for the same reason.

(2) Impact forces are very high and of short duration, therefore the impulse of external forces such as solar pressure, is negligible. Due to the short duration of impacts, it is assumed that there is no considerable change in the system configuration during an impact, i.e. joint rotations during the impact are considered negligible. This applies also in the zero-g environment even if there is no fixed base, because each joint appears as fixed in a position in space during an impact due to the inertia of the system bodies involved in the impact ("*quasi-static*"). Finally,

(3) Relative velocities between bodies are within the limits of low speed impacts; i.e. no impacts with plastic effects are considered.

Some of these assumptions are typical when dealing with impact models (Stronge, 2000). No other requirement is set for the exact impact model or the coefficient of restitution. Manipulator workspace and singularity issues are out of the scope of this work. For the duration of both the impact and the simulations in this work, orbital mechanics effects are also negligible.

2.2. The concept of the Centre of Percussion

The CoP is a property of bodies able to rotate about a fixed axis. If an impact occurs at the CoP, the reaction force exerted on the fixed rotation axis (i.e. on the bearings of the rotational joint), tends to a minimum including zero. More specifically, let a beam, see Fig. 1, that can rotate about a Rotation Axis (RA). An impact occurs at a point on the longitudinal axis. Then, the overall movement of the body consists of the superposition of (i) a translation in the direction of the impulse, with an inertial force exerted at its RA and (ii) a rotation about its Centre of Mass (CM), with an inertial force applied to the RA. Here, the magnitude of the latter is related to the relative position of the impact point with respect to the CM, whereas its direction is opposite to the reaction force due to translation. If the impact occurs at the CoP the magnitude of the latter reaction force is equal to the magnitude of the reaction force exerted due to the translation. Therefore in this case the vectorial sum of the forces exerted on the RA is zero – at least in principle.

2.3. Centre of Percussion for 2D systems

To study the CoP concept analytically, consider the free body diagram in Fig. 2. Assume an impact force is applied at some point (impact point-IP) along the longitudinal axis. For purposes of generality, the impact force can have any direction. Balance of forces and moments yield,

$$-m\dot{v}_{cm}\sin\theta = -m\ddot{\theta}r_{cm}\cos\theta = N_x - F_{imp}\cos(\phi+\theta) \quad (1)$$

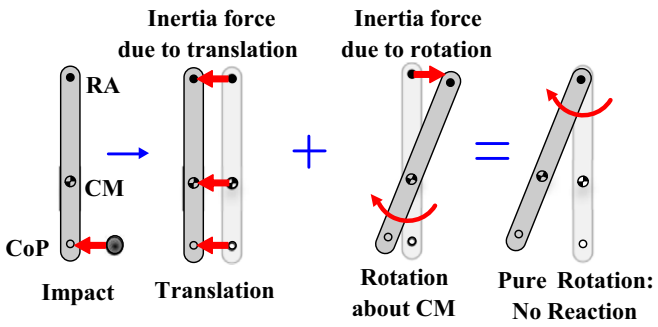

Fig. 1. The concept of CoP: elimination of reaction forces.

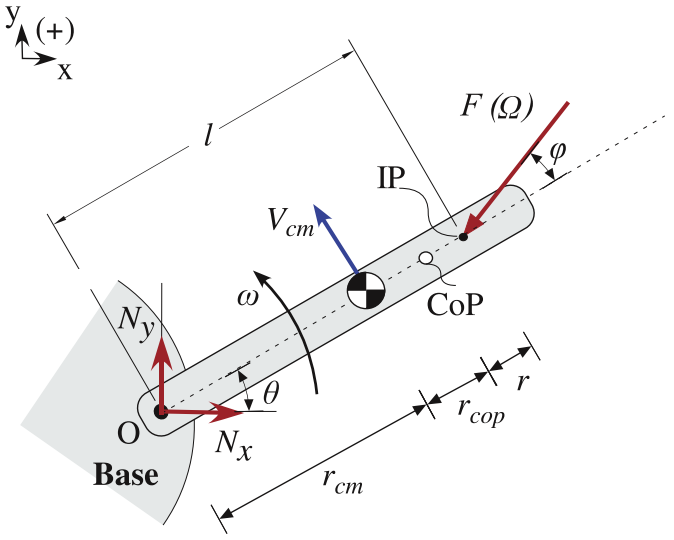

Fig. 2. Free body diagram of a beam under impact force.

$$m\dot{v}_{cm}\cos\theta = m\ddot{\theta}r_{cm}\cos\theta = N_y - F_{imp}\sin(\phi+\theta) \tag{2}$$

$$I^o\ddot{\theta} = -lF_{imp}\sin\phi \tag{3}$$

where all symbols are defined in Fig. 2 and m is the mass of the body. The body polar inertia I^o about the RA at O is,

$$I^o = I^c + mr_{cm}^2 \tag{4}$$

The impact point is located at distance

$$l = l_{cop} + r = (r_{cop} + r_{cm}) + r \tag{5}$$

from joint O, where r is the displacement of IP from the CoP (negative if the displacement is towards the CM and positive otherwise). Integrating (1)–(3) for infinitesimal time, the forces result in impulses and the accelerations in velocities, e.g. for the reaction force, the corresponding impulse is

$$\Omega_{Nx} = \lim_{\varepsilon\to 0}\int_0^{\varepsilon} N_x\,dt \tag{6}$$

where ε is the duration of the impact. Other variables, including rotation angle and impact angle, remain unchanged due to assumption (2).

After some algebraic manipulation and applying trigonometric identities, the magnitude of the impulse of the reaction force N, Ω_N, is given by

$$\Omega_N^2 = \Omega_{Nx}^2 + \Omega_{Ny}^2 = \Omega_{F_{imp}}^2\left[1 + \left(C_{ID}^2 - 2C_{ID}\right)\sin^2\phi\right] \tag{7}$$

with

$$C_{ID} = lr_{cm}m\left(I^o\right)^{-1} \tag{8}$$

where C_{ID} is the *Coefficient of Impact Design*, a coefficient which relates the physical characteristics of the body to the location of the impact. Equations are simplified using the non-dimensional impulse $\tilde{\Omega}_N$,

$$\tilde{\Omega}_N = \sqrt{\Omega_N^2/\Omega_{F_{imp}}^2} \tag{9}$$

Eq. (7) does not depend on the beam angle θ, but depends on the angle of impact ϕ, and the IP and body parameters due to (8). To find the CoP, the reaction impulse is zeroed, yielding

$$\tilde{\Omega}_N = 0 \Leftrightarrow \phi = \pm\sin^{-1}\left[\left(2C_{ID} - C_{ID}^2\right)^{-1/2}\right] = \pm\sin^{-1}\beta \tag{10}$$

The term in the brackets is valid for $\beta \le 1$, while the radicand of the square root has real values only for $0 < C_{ID} < 2$, and thus $\beta \ge 1$. Therefore, the reaction impulse will be eliminated if and only if

$$\tilde{\Omega}_N = 0 \Leftrightarrow \beta = 1 \Leftrightarrow C_{ID} = 1 \text{ and } \phi = \pm\pi/2 \tag{11}$$

The sign is related to the force direction. Eq. (11) shows the uniqueness of the CoP along the longitudinal axis of a beam for a rigid body. From (8), and using (4), (5) and (11) for $r = 0$ (impact occurs at the CoP), it can be found that the CoP's location r_{cop} is given by

$$C_{ID} = lr_{cm}m\left(I^o\right)^{-1} = 1 \Leftrightarrow$$
$$\Leftrightarrow r_{cop} = I^c\left(r_{cm}m\right)^{-1} \tag{12}$$

Interestingly, if $r_{cm} \to 0 \Leftrightarrow r_{cop} \to +\infty$, i.e. the reaction forces cannot be eliminated on a statically balanced body. On the other hand if $r_{cm} \to +\infty \Leftrightarrow r_{cop} \to 0$, i.e. on a body with all its mass concentrated at a point away from the RA, the CoP is at the same point. Using (11) and (7), and when $\phi \neq \pm\pi/2$, one can see that in this case the non-dimensional impulse cannot be zeroed; this is because in such a case there is always an impact force component parallel to the longitudinal axis, whose line of action passes through O and therefore does not produce any moment about the RA. Thus it acts directly on the joint axis, and this cannot be cancelled, see also Fig. 1.

2.4. Centre of Percussion for 3D systems

Consider the rigid body in Fig. 3, whose Centre of Rotation (CR) is located at the spherical joint O, and a force $\mathbf{F}_{imp}$ acting on it at an Impact Point (IP).

The equations of motion for the Coordinate System (CS) a: $\{xyz\}$ are

$$\sum {}^a\mathbf{F}_o = m{}^a\dot{\mathbf{v}}_{cm} = {}^a\mathbf{N} + {}^a\mathbf{F}_{imp} \tag{13}$$

$$\sum {}^a\mathbf{M}_o = d/dt\left({}^a\mathbf{I}^o\,{}^a\omega\right) = \left({}^a\mathbf{l}_{imp} \times {}^a\mathbf{F}_{imp}\right) \tag{14}$$

where $\mathbf{N}$ is the reaction force at O, $\mathbf{I}^o$ is the inertia matrix of the body with respect to O, $\mathbf{F}_o$ and $\mathbf{M}_o$ is the vectorial sum of forces and moments with respect to O correspondingly, $\mathbf{v}_{cm}$ is the linear velocity of the CM and $\boldsymbol{\omega}$ is the angular velocity of the body around O. The left superscript refers to a vector expressed in the CS a. For any CS, the following holds ($\mathbf{1}_3$ is the 3×3 unit matrix)

$$\mathbf{v}_{cm} = \boldsymbol{\omega} \times \mathbf{r}_{cm} \tag{15}$$

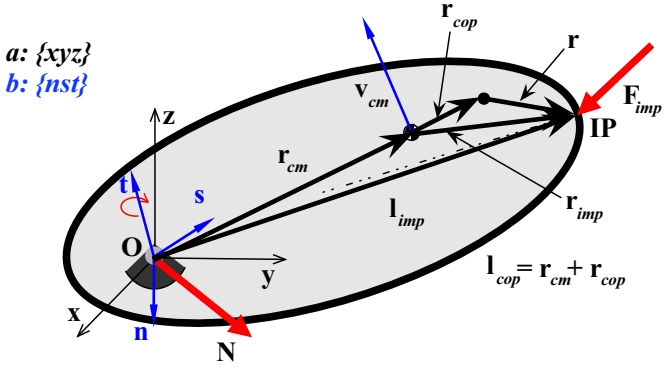

Fig. 3. A 3D rigid body rotating around a spherical joint and the geometrical elements used to derive the CoP conditions in the 3D case.

$$\mathbf{l}_{imp} = \mathbf{r}_{cm} + \mathbf{r}_{imp} = \mathbf{r}_{cm} + \mathbf{r}_{cop} + \mathbf{r} = \mathbf{l}_{cop} + \mathbf{r} \tag{16}$$

$$\mathbf{I}^o = \mathbf{I}^c + m\left(\left(\mathbf{r}_{cm}^T\mathbf{r}_{cm}\right)\mathbf{1}_3 - \mathbf{r}_{cm}\mathbf{r}_{cm}^T\right) \tag{17}$$

where $\mathbf{I}^c$ is the inertia matrix with respect to the CM, and all vectors are defined in Fig. 3. Integrating (13) and (14) for a short duration, using (15), and performing some algebraic manipulation results in

$${}^a\mathbf{I}^o\,{}^a\boldsymbol{\omega} = \left[{}^a\mathbf{l}_{imp} \times \left(m\,{}^a\boldsymbol{\omega} \times {}^a\mathbf{r}_{cm} - {}^a\boldsymbol{\Omega}_N\right)\right] \tag{18}$$

where ${}^a\boldsymbol{\Omega}_N$ is the reaction impulse at point O.

The impact force $\mathbf{F}_{imp}$ and the corresponding reaction force $\mathbf{N}$ can be considered as the vectorial sum of normal components $\mathbf{F}_{imp\perp}$ and $\mathbf{N}_\perp$, and parallel components $\mathbf{F}_{imp\parallel}$ and $\mathbf{N}_\parallel$ to the impact vector $\mathbf{l}_{imp}$, irrespective of the CS. The same stands for their corresponding impulses therefore

$$\boldsymbol{\Omega}_{F_{imp}} = \boldsymbol{\Omega}_{F_{imp}\perp} + \boldsymbol{\Omega}_{F_{imp}\parallel} \tag{19}$$

$$\boldsymbol{\Omega}_N = \boldsymbol{\Omega}_{N\perp} + \boldsymbol{\Omega}_{N\parallel} \tag{20}$$

The parallel component $\boldsymbol{\Omega}_{N\parallel}$, which corresponds to the reaction of the parallel component $\boldsymbol{\Omega}_{F_{imp}\parallel}$ cannot be eliminated. This is because $\mathbf{F}_{imp\parallel}$ does not produce a moment around O and its line of action passes through the CR. Therefore, the aim is to eliminate the $\boldsymbol{\Omega}_{N\perp}$ due to $\mathbf{F}_{imp\perp}$. This requirement can be summarised as the inner product

$$\mathbf{l}_{imp}\cdot\mathbf{F}_{imp\perp} = 0 \tag{21}$$

Note that (21) is valid for any CS. This condition is qualitatively similar to the angle requirement in (11). Using (20) in (18), and given that the cross product of parallel vectors is zero, one finds that,

$${}^a\mathbf{I}^o\,{}^a\boldsymbol{\omega} - {}^a\mathbf{l}_{imp} \times \left(m\,{}^a\boldsymbol{\omega} \times {}^a\mathbf{r}_{cm}\right) = {}^a\boldsymbol{\Omega}_{N\perp} \times {}^a\mathbf{l}_{imp} \tag{22}$$

To eliminate $\boldsymbol{\Omega}_{N\perp}$, it is required that the left side of (22) must be equal to zero (${}^a\mathbf{l}_{imp} \neq \mathbf{0}$ otherwise the impact occurs at the spherical joint). According to the definition of the CoP, for such a point, ${}^a\mathbf{l}_{imp} = {}^a\mathbf{l}_{cop}$, and therefore

$${}^a\mathbf{I}^o\,{}^a\boldsymbol{\omega} = {}^a\mathbf{l}_{cop} \times \left(m\,{}^a\boldsymbol{\omega} \times {}^a\mathbf{r}_{cm}\right) \Leftrightarrow$$

$$\Leftrightarrow {}^a\mathbf{I}^o\,{}^a\boldsymbol{\omega} = m\left({}^a\mathbf{r}_{cm} \times {}^a\boldsymbol{\omega}\right) \times {}^a\mathbf{l}_{cop} \tag{23}$$

During an impact, the moment with respect to CS a due to $\mathbf{F}_{imp}$ is defined as

$${}^a\mathbf{M} = {}^a\mathbf{l}_{imp} \times {}^a\mathbf{F}_{imp} \tag{24}$$

Thus the instantaneous axis of rotation is given by

$$\hat{\mathbf{t}} = {}^a\mathbf{M}/\|{}^a\mathbf{M}\| \tag{25}$$

Let also unit vectors $\hat{\mathbf{n}}$ and $\hat{\mathbf{s}}$ be normal to each other and to $\hat{\mathbf{t}}$ so that an orthogonal CS b: $\{nst\}$ is formed (the $\hat{\mathbf{n}}$ or the $\hat{\mathbf{s}}$ correspond to any arbitrary direction on the $\{ns\}$ plane as long as they are perpendicular to each other and to $\hat{\mathbf{t}}$). The instantaneous angular velocity in this CS is then

$${}^b\boldsymbol{\omega} = \begin{pmatrix}0 & 0 & \omega_t\end{pmatrix}^T \tag{26}$$

It will be advantageous to write (23) as

$${}^a\mathbf{I}^o\,{}^a\boldsymbol{\omega} = m\,{}^a\mathbf{r}_{cm}^{\times}\,{}^a\boldsymbol{\omega}_{\times}\,{}^a\mathbf{l}_{cop} \tag{27}$$

where $\mathbf{r}^\times$ is the matrix that corresponds to a cross product

$$\mathbf{r} = \begin{pmatrix}x & y & z\end{pmatrix} \Leftrightarrow \mathbf{r}^{\times} = \begin{pmatrix}0 & -z & y\\ z & 0 & -x\\ -y & x & 0\end{pmatrix} \tag{28}$$

Eq. (27) written in CS b becomes

$${}^b\mathbf{I}^o\,{}^b\boldsymbol{\omega} = m\,{}^b\mathbf{r}_{cm}^{\times}\,{}^b\boldsymbol{\omega}^{x b}\mathbf{l}_{cop} \tag{29}$$

Eq. (29) using (26) and a generic inertia matrix

$${}^b\mathbf{I}^o = \begin{pmatrix}{}^bI^o_{nn} & {}^bI^o_{ns} & {}^bI^o_{nt}\\ {}^bI^o_{sn} & {}^bI^o_{ss} & {}^bI^o_{st}\\ {}^bI^o_{tn} & {}^bI^o_{ts} & {}^bI^o_{tt}\end{pmatrix} \tag{30}$$

yields

$$\omega_t\begin{pmatrix}{}^bI^o_{nt} + mr_{cm,t}l_{cop,n}\\ {}^bI^o_{st} + mr_{cm,t}l_{cop,s}\\ {}^bI^o_{tt} - m\left(r_{cm,s}l_{cop,s} + r_{cm,n}l_{cop,n}\right)\end{pmatrix} = \mathbf{0} \tag{31}$$

where $r_{cm,(i=n,s,t)}$ and $l_{cop,(i=n,s,t)}$ refer to the i component of the corresponding vector in CS b. For (23) to be valid, the column vector in (31) must be zero. The case where $\omega_t = 0$ is trivial (no impact occurs). Therefore, (31) holds if all of the following conditions hold:

(i) $\hat{\mathbf{t}}$ is a principal inertia axis of the body. Then,

$${}^bI^o_{nt} = {}^bI^o_{st} = 0 \tag{32}$$

(ii) There is symmetry in mass distribution with respect to the $\{ns\}$ plane, i.e.

$$r_{cm,t} = 0 \tag{33}$$

(iii) Using the last row of (31) and (33), the impact occurs at a point, which satisfies

$${}^b\mathbf{r}_{cm}\cdot{}^b\mathbf{l}_{cop} = {}^bI^o_{tt}m^{-1} \tag{34}$$

which by virtue of (16) and (17), and (33) becomes

$${}^b\mathbf{r}_{cm}\cdot{}^b\mathbf{r}_{cop} = {}^bI^c_{tt}m^{-1} \tag{35}$$

Eq. (35) requires that the IP, the CM and the CR should be collinear. In the planar case, $\hat{\mathbf{t}}$ is substituted with $\hat{\mathbf{z}}$, and (35) reduces to (12). It is reminded that (21) should also apply. On the other hand if only (21) and (35) apply, the reaction forces can be still reduced but not eliminated (note that in this case (35) applies for the projection of the CM on the $\{ns\}$ plane). From the analysis of the 3D case, one can deduce that in order to eliminate the reaction forces on the spherical joint, the impact should occur in certain planes, rendering the problem essentially planar. Therefore for the rest of this work it is assumed that impacts occur in a plane, for which, the reaction forces can be eliminated.

3. Robustness to parametric uncertainties

3.1. Introduction

As described in Section 2, the minimization of the reaction is possible either in the planar case, or at specific planes in the three dimensional case. The analysis here will focus to the planar case and necessary adaptations for the 3D case will be presented later.

It is important to examine the effects of deviations in the angle ϕ or the C_{ID} on the rate of change of the non-dimensional impulse given by (7). Fig. 4a displays $\partial(\bar{\Omega}_N)/\partial\phi$ as a function of ϕ. It can be

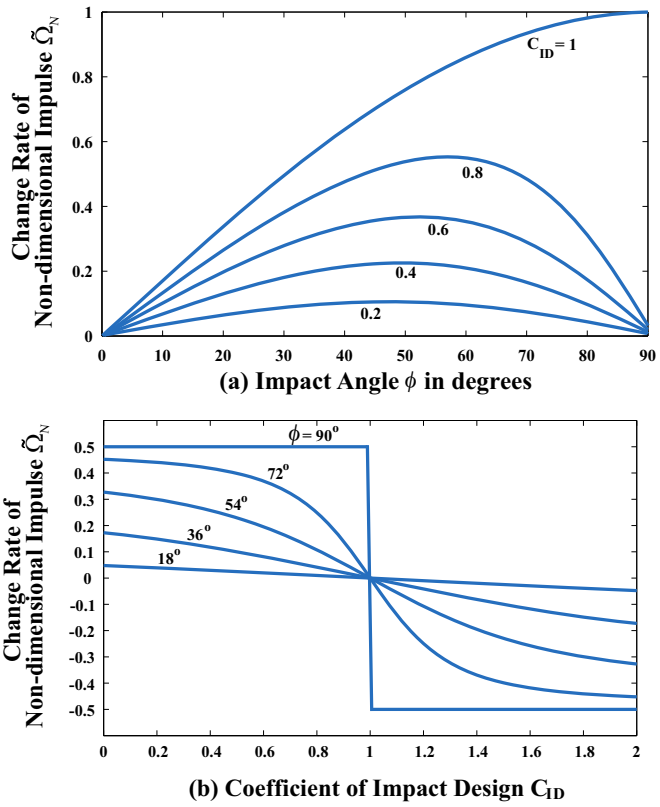

Fig. 4. Change rate of non-dimensional impulse as (a) impact angle changes and (b) as the coefficient of impact design changes.

seen that the sensitivity is highest when $C_{ID}=1$. Similarly Fig. 4b shows $\partial(\tilde{\Omega}_N)/\partial C_{ID}$ as a function of C_{ID}. It is observed that the highest sensitivity is at $\phi=90°$; however it is constant throughout the range of C_{ID}. This is expected, as in this case, the parallel component of the impact force is the only part that cannot be compensated and is not affected by the IP. This preliminary sensitivity analysis shows that deviations from the normal impact angle yield higher rate of change of the reaction forces than deviations from the impact location of the CoP. Therefore prior to an impact, a system should assume a configuration which allows fulfilment of the requirements of the CoP as in (11); if this cannot be achieved, then the angle of the impact should be kept as close to $\phi=90°$ as possible. Next, the way deviations of system or impact parameters affect the reaction forces is examined more precisely.

3.2. Non-dimensional analysis of the uncertainties

To analyse further the effects of the deviation of an IP from the CoP, $\tilde{r}$ is defined as the non-dimensional displacement from the CoP, see Fig. 2.

$$\tilde{r}=r/r_{cop} \tag{36}$$

where r is the distance of the IP from the CoP. Additionally the notion of the "*impact configuration*" is defined as "*the set of system and impact parameters prior to an impact, necessary to describe the impact behaviour*".

In this context the system parameters include the body parameters in the C_{ID}, and the impact parameters include the impact distance $\tilde{r}$ and impact angle ϕ.

Assume next that an upper limit for the non-dimensional impulse $\tilde{\Omega}_N$ has been set. One can define two extreme bounds:

a) The *minimum impact angle*, $\phi_{\min}$, defined if and only if the impact occurs at the CoP. More specifically for an impact at the CoP ($C_{ID}=1$), and for a given $\tilde{\Omega}_N$, (7) results in:

$$\left(\tilde{\Omega}_N\right)^2=1-\sin^2\phi_{\min}\Rightarrow\phi_{\min}=\sin^{-1}\left(\left(1-\left(\tilde{\Omega}_N\right)^2\right)^{1/2}\right) \tag{37}$$

b) The *maximum distance of the IP from the CoP*, defined non-dimensionally by $C_{ID\,\max}$, if and only if the impact force is normal to the longitudinal axis of the body (as defined by the line that connects the RA and the CoM). For a normal impact ($\phi=90°$) and for a given $\tilde{\Omega}_N$, one can find from (7):

$$C^{\pm}_{ID\,\max}=1\pm\tilde{\Omega}_N \tag{38}$$

The next question to focus on is, for a given $\tilde{\Omega}_N$ what impact configurations are admissible (i.e. impact point distance and impact angle). Note that the impact angle cannot be eliminated; that would mean that the impact is collinear to the longitudinal axis and that no reaction reduction measure can be applied to the joint under consideration. Values of $C^{+}_{ID\,\max}>2$ or $C^{-}_{ID\,\max}<0$ are of no interest, as in this case the reaction force due to the developed moment becomes larger than the impact force, see also (7); in fact in this case the joint acts like a fulcrum.

Using (7), one can find the dependence of C_{ID} by the non-dimensional impulse and the impact angle as

$$\left(\tilde{\Omega}_N\right)^2=1+\left[\left(C_{ID}{}^2-2\,C_{ID}\right)\sin^2\phi\right]\overset{(\phi\neq k\cdot\pi,k\ni\mathbb{Z})}{\Rightarrow}$$

$$\Rightarrow C_{ID}{}^2-2\,C_{ID}-\left(\left(\tilde{\Omega}_N\right)^2-1\right)\left(\sin^2\phi\right)^{-1}=0\Rightarrow$$

$$\Rightarrow C_{ID}=1\pm\sqrt{1-\left(\left(\tilde{\Omega}_N\right)^2-1\right)\left(\sin^2\phi\right)^{-1}} \tag{39}$$

Eq. (39) is being plotted for a given $\tilde{\Omega}_N$ in Fig. 5. Every impact configuration inside the sketched area results in a reaction force less than $\tilde{\Omega}_N$. Therefore considering the uncertainties of the body characteristics and the impact point – thus the C_{ID}, and the uncertainties on the impact angle estimation – thus the ϕ, one can estimate how close an impact configuration is to the limits of the sketched area, where the non-dimensional impulse equals to $\tilde{\Omega}_N$. In this way, the impact configuration (represented by its nominal point and estimated errors) for a system, which is closer to the limits of Fig. 5, is the limiting case for impact for this system.

3.3. Assessment of performance during design

The relationship between C_{ID}, ϕ and $\tilde{\Omega}_N$ can be studied using Fig. 6, in which lines of constant impact angles have been drawn. The areas outside the lines of $\phi=90°$ cannot be achieved. Fig. 6

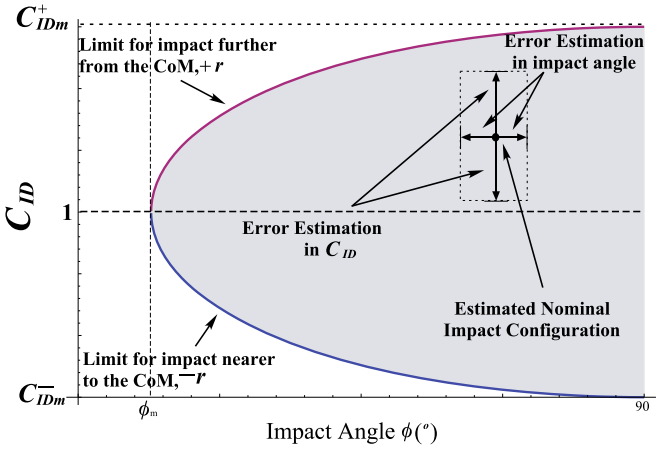

Fig. 5. Graph of feasible impacts for a defined $\tilde{\Omega}_N$.

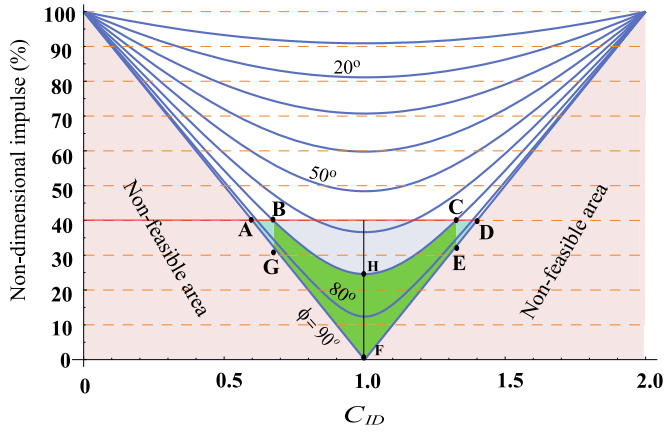

Fig. 6. Graph of feasible impacts and example.

can be used also for the estimation of body parameters during the design phase or for estimating the performance under known impacts. More specifically, (8) is rewritten using (36) thus

$$C_{ID} = lmr_{cm}\left(I^o\right)^{-1} = 1 + C_{MD}\tilde{r} \tag{40}$$

where C_{MD} is the *Coefficient of Mass Distribution* defined as the ratio between the body polar inertia with respect to its CM, I^c, to the body polar inertia with respect to the RA, I^o.

The C_{MD} is a metric for the "symmetry" of the mass distribution between the CM and the RA. To clarify this further, note that,

$$C_{MD} = I^c/I^o = I^c\left(I^c + mr_{cm}^2\right)^{-1} \Rightarrow 0 \le C_{MD} \le 1 \tag{41}$$

thus it can be seen that as the CM is closer to the RA ($r_{cm} \to 0$), there is larger "symmetry" in the mass distribution ($C_{MD} = 1$), whereas as the RA is further away from the CM ($r_{cm} \to +\infty$), this "symmetry" is affected ($C_{MD} \to 0$).

As an example of the use of Fig. 6, suppose that the control designer sets the following limits for nominal operation of a manipulator during impacts: $\phi = 70°$ and $\tilde{\Omega}_N = 0.4$. One can find that the given ϕ and $\tilde{\Omega}_N$ correspond to point B (and C) and from the graph, this corresponds to $C_{ID} = 0.68$ (and $C_{ID} = 1.32$). Knowing the parameters of the system, thus the C_{MD}, the maximum deviation of the IP from the CoP can be found – and eventually the acceptable level of uncertainty during the impact.

One can recognise the following areas in Fig. 6: (i) BHCEFGB is the area for which any impact is within the requirements, (ii) BCHB is an area in which the $\tilde{\Omega}_N$ satisfies the requirements, while the angle requirement is relaxed, provided however that the IP is nearer to the CoP. Finally, (iii) ABGA and CDEC are areas in which the $\tilde{\Omega}_N$ requirement is met, but the impact angle must be greater than the minimum requirement. Therefore, in the case in which the body parameters are known, using the abovementioned method it is possible to tune a controller's performance according to the required limits of the task. Apparently the stricter the requirements are with respect to the given impulse limits, the more robust the controller should be.

3.4. Extensions to the 3D case

Here, the interest lies in the plane normal to the instantaneous axis of rotation $\hat{\mathbf{t}}$ according to CS b: $\{nst\}$, Fig. 3. Therefore the $C_{ID,t}$ is the *Coefficient of Impact Design about* $\hat{\mathbf{t}}$, which relates the physical characteristics of the body to the location of the impact

$$C_{ID,t} = m\left({}^bI_{tt}^o\right)^{-1}{}^b\mathbf{l}\cdot{}^b\mathbf{r}_{cm} \tag{42}$$

where ${}^b\mathbf{l}$ is the vector which connects the IP and the RA, ${}^b\mathbf{r}_{cm}$ is the vector which connects the CM and the RA, m is the mass of the body and ${}^bI_{tt}^o$ the body polar inertia about $\hat{\mathbf{t}}$. Additionally the *Coefficient of Mass Distribution about* $\hat{\mathbf{t}}$ is

$$C_{MD,t} = {}^bI_{tt}^c/{}^bI_{tt}^o \tag{43}$$

which is the ratio between the body polar inertia with respect to its CM about $\hat{\mathbf{t}}$, ${}^bI_{tt}^c$, and the body polar inertia with respect to the RA about $\hat{\mathbf{t}}$, ${}^bI_{tt}^o$. Finally the deviation of the IP from the CoP $\tilde{r}_t$ is the non-dimensional deviation from CoP

$$\tilde{r}_t = \mathrm{sgn}\left({}^b\mathbf{r}\cdot{}^b\mathbf{r}_{cm}\right)\frac{\|{}^b\mathbf{r}\cdot{}^b\mathbf{r}_{cm}\|}{\|{}^b\mathbf{r}_{cop}\cdot{}^b\mathbf{r}_{cm}\|} \tag{44}$$

where ${}^b\mathbf{r}$ is the vector which connects the IP with the CoP. By applying the above definitions, the rest of the planar analysis for the robustness during parametric uncertainties is valid for the 3D case.

4. Impact compensation using CoP

4.1. CoP for multibody manipulators

To examine the effects of the CoP in robotic systems, it is useful to derive the CoP for multibody systems. For completeness, the necessary analysis based on our previous work (Paraskevas & Papadopoulos, 2013) is presented briefly.

In Fig. 7, the external impact force $\mathbf{f}_{imp,i}$ acts on the impact point (IP), which is located at $\mathbf{r}_{un,i}$ from CM and $-\mathbf{r}_{dist,i}$ from next joint $\{i+1\}$. The ${}^i\mathbf{r}_{cop,i}$ is the vector from CM to the CoP and ${}^i\mathbf{r}_i$ is the vector from the CoP to the IP; the remaining vectors are defined in Fig. 7.

Using the Newton–Euler Algorithm (NEA) for two adjacent links, in a impulse form (Paraskevas & Papadopoulos, 2013; Craig, 2004). the following results

$$\begin{aligned}\left({}^i\mathbf{r}_{C,i} + {}^i\mathbf{r}_{un,i}\right)^{\times}{}^i\boldsymbol{\Omega}_{\mathbf{f},i} = \\ = \underbrace{\left[\left({}^i\mathbf{r}_{cop,i} + {}^i\mathbf{r}_i\right)^{\times} m_i\left({}^i\boldsymbol{\omega}_i^{\times}{}^i\mathbf{r}_{C,i}\right) - {}^{C,i}\mathbf{I}_i^i\boldsymbol{\omega}_i\right]}_{A} - \\ - \underbrace{\left[{}^i\mathbf{r}_{dist,i}^{\times}\left({}^i\mathbf{R}_{i+1}{}^{i+1}\boldsymbol{\Omega}_{\mathbf{f},i+1}\right)\right]}_{B} + \\ + \underbrace{\left[{}^i\mathbf{r}_{un,i}^{\times}\left(m_i{}^i\mathbf{v}_i\right)\right]}_{C} + \underbrace{\left[\int\left({}^i\mathbf{n}_i - {}^i\mathbf{R}_{i+1}{}^{i+1}\mathbf{n}_{i+1}\right)\right]}_{D}\end{aligned} \tag{45}$$

where ${}^i\boldsymbol{\Omega}_{\mathbf{f},i}$ is the reaction impulse at joint $\{i\}$.

To obtain ${}^i\boldsymbol{\Omega}_{\mathbf{f},i} = 0$, the right side of (45) should be zero. In the

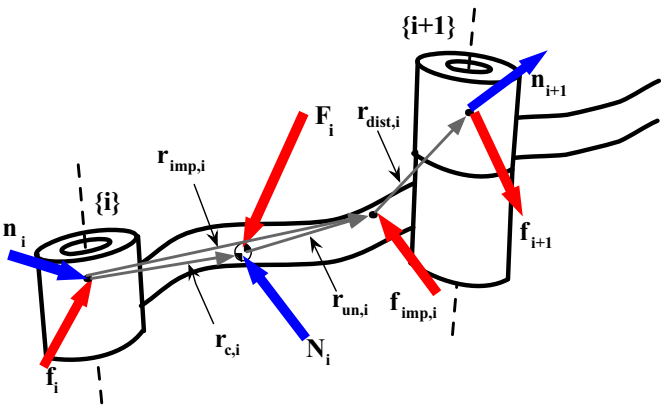

Fig. 7. Free body diagram of two adjacent manipulator links.

case where the rotational joints are free, (zero friction is assumed), then $D = 0$. Due to the *quasi-static* assumption, $C = 0$. Two cases are possible for a robot with N links:

(i) The joint is on the last link of the robot $(i = N)$-then $B = 0$. Using (17) and (29) the following applies

$$ {}^{b}\mathbf{I}^{c}\,{}^{b}\boldsymbol{\omega} = m\,{}^{b}\mathbf{r}_{cm}^{\times}\,{}^{b}\boldsymbol{\omega}_{\times}\,{}^{b}\mathbf{r}_{cop} \tag{46} $$

therefore for (45) to apply, the following must hold

$$ m_i^i\mathbf{r}_i^{\times}\left({}^{i}\boldsymbol{\omega}_i^{\times i}\mathbf{r}_{C,i}\right) = 0 \tag{47} $$

or in other words, ${}^{i}\mathbf{r}_i$ must be zero and the impact must occur at the CoP. If this is not the case, reaction forces develop, as already discussed in Section 3.

(ii) In the general case in which $(i \neq N)$, the following must apply

$$ \underbrace{\left[\left({}^{i}\mathbf{r}_{cop,i} + {}^{i}\mathbf{r}_i\right)^{\times} m_i\left({}^{i}\boldsymbol{\omega}_i^{\times i}\mathbf{r}_{C,i}\right) - {}^{C,i}\mathbf{I}_i\,{}^{i}\boldsymbol{\omega}_i\right]}_{A} - \underbrace{\left[{}^{i}\mathbf{r}_{dist,i}^{\times}\left({}^{i}\mathbf{R}_{i+1}\,{}^{i+1}\boldsymbol{\Omega}_{\mathbf{f},i+1}\right)\right]}_{B} = \mathbf{0} \tag{48} $$

In this case, $A - B = 0$. This means that if the reaction from joint $\{i+1\}$ and an impact force $\mathbf{f}_{imp,i}$ act simultaneously and directly on link $\{i\}$, it is possible to eliminate the reaction on joint $\{i\}$. A more common and useful case is when the impact force acts only at the end effector (link N), while the previous rotational joints $\{i < N\}$ must cope with the reaction forces, which propagate. In this case it is easy to see that if the joint $\{i+1\}$ is on the CoP of link $\{i\}$ then ${}^{i}\mathbf{r}_{dist,i} = {}^{i}\mathbf{r}_i = 0$ and thus $A = B = 0$.

The above analysis concludes that in order to minimize reaction forces on joint bearings, it is best to position the revolute joints on the CoP of the previous link, while the impact should occur at the CoP of the last link.

If $D \neq 0$, (45) can be eliminated if the following applies

$$ {}^{i}\mathbf{r}_i^{\times}\, m_i\left({}^{i}\boldsymbol{\omega}_i^{\times}\,{}^{i}\mathbf{r}_{C,i}\right) + \int\left({}^{i}\mathbf{n}_i - {}^{i}\mathbf{R}_{i+1}\,{}^{i+1}\mathbf{n}_{i+1}\right) = 0 \tag{49} $$

where ${}^{i}\mathbf{r}_i$ is the distance of the joint $\{i+1\}$ (or the IP for the last link, normally this point is the end effector point) from the CoP of link $\{i\}$. If link $\{i\}$ is subject to several impacts including the reaction of joint $\{i+1\}$, (49) is valid using the vectorial sum of all impact forces at ${}^{i}\mathbf{r}_i$, while an external moment is added to the integral.

4.2. Impact Compensation using CoP (IC^2)

In case the rotational joints are not free, (49) can be used to examine if the reaction forces can be reduced by motor actuation. First the case where the joints are completely frictionless is examined. The ${}^{i}\mathbf{n}_i$ is substituted with ${}^{i}\mathbf{n}_{cop,i}$ for convenience, therefore from (49) the following applies,

$$ \int {}^{i}\mathbf{n}_{cop,i} = -\,{}^{i}\mathbf{r}_i^{\times}\, m_i\left({}^{i}\boldsymbol{\omega}_i^{\times}\,{}^{i}\mathbf{r}_{C,i}\right) + \int\left({}^{i}\mathbf{R}_{i+1}\,{}^{i+1}\mathbf{n}_{i+1}\right) \tag{50} $$

Noting that for the small duration of the impact, only the angular velocity and the impulse are affected, (50), yields,

$$ {}^{i}\mathbf{n}_{cop,i} = -\,{}^{i}\mathbf{r}_i^{\times}\, m_i\left({}^{i}\dot{\boldsymbol{\omega}}_i^{\times}\,{}^{i}\mathbf{r}_{C,i}\right) + {}^{i}\mathbf{R}_{i+1}\,{}^{i+1}\mathbf{n}_{i+1} \tag{51} $$

where ${}^{i}\mathbf{r}_i$ locates the joint $\{i+1\}$, or the IP with respect to the CoP of link $\{i\}$. Note that if $i = N$, $\{i\}$ is the last link of the robotic arm, and (51) is simplified to

$$ {}^{i}\mathbf{n}_{cop,i} = -\,{}^{i}\mathbf{r}_i^{\times}\, m_i\left({}^{i}\dot{\boldsymbol{\omega}}_i^{\times}\,{}^{i}\mathbf{r}_{C,i}\right) \tag{52} $$

whereas if $i \neq N$ but joint $\{i+1\}$ is located at the CoP of link $\{i\}$, then

$$ {}^{i}\mathbf{n}_{cop,i} = {}^{i}\mathbf{R}_{i+1}\,{}^{i+1}\mathbf{n}_{i+1} \tag{53} $$

Eqs. (51)–(53) provide the necessary motor torque in order to compensate an impact, which occurs at a point different than the CoP of the last link, and to compensate for the reaction forces propagated by the successive links and joints. Note that in the case of the space robot base an equal torque to the torque applied to the next joint $\{1\}$ must be applied by the actuators of the base, otherwise due to the dynamic coupling, reaction forces are developed at joint $\{1\}$ which back-propagate. That is control action must be applied to all rotational joints including the base. Naturally (51)–(53) cannot provide any compensation for the component of the force whose line of action passes through the joint location.

Additionally it is important to consider that for (51)–(53) to be effective, given that the impact is a process with fast dynamics, it is necessary to compensate joint friction. Otherwise the compensation torque based on the CoP will not be exact, because friction will apply an undesired torque opposing the motor-induced motion. Therefore, the motor must apply a friction compensation torque at each joint (Nef & Lum, 2009) i.e. a torque ${}^{i}\mathbf{n}_i$, which is of the form

$$ {}^{i}\mathbf{n}_i = {}^{i}\mathbf{n}_{cop,i} + {}^{i}\mathbf{n}_{fr,i} \tag{54} $$

where ${}^{i}\mathbf{n}_{cop,i}$ is the control torque calculated in (51)–(53) and ${}^{i}\mathbf{n}_{fr,i}$ is the friction compensation torque. To calculate this torque, a number of friction models can be used (Papadopoulos & Chasparis, 2004; Åström & Canudas-de-wit, 2008).

To implement the IC^2 controller, the following scheme is proposed. Let a space robot whose dynamics are described by,

$$ \boldsymbol{\tau} = \mathbf{M}\,\ddot{\mathbf{q}} + \mathbf{V}(\mathbf{q}, \dot{\mathbf{q}}) + \mathbf{J}^{T}\mathbf{F} \tag{55} $$

where $\mathbf{q}$ is the vector of joint variables, $\boldsymbol{\tau}$ is the vector of all actuator forces and torques, $\mathbf{M}$ is the configuration-dependent mass matrix, $\mathbf{V}(\mathbf{q}, \dot{\mathbf{q}})$ is the vector of nonlinear velocity terms and $\mathbf{J}^{T}\mathbf{F}$ resolves the effects of external impact forces $\mathbf{F}$ to each joint,

The developed IC^2 controller acts during the impact; after external impact force elimination, and thus elimination of the impact joint reactions, the control system switches to the normal system controller e.g. to a model-based controller which moves the end effector to a desired position, see Fig. 8.

Thus the proposed control methodology is a two-part one. First, the robot motion is controlled e.g. by a model based controller,

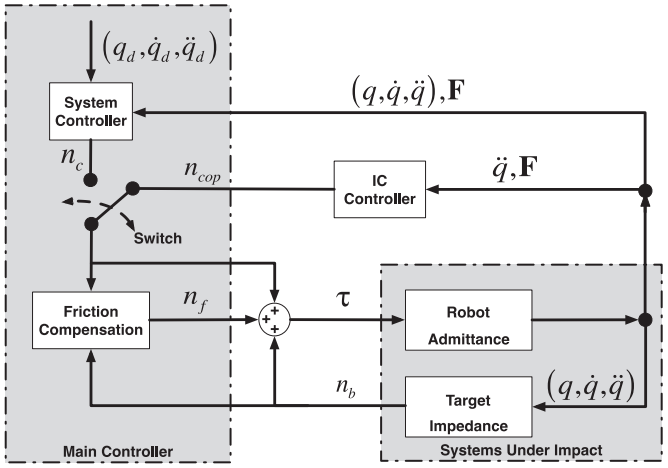

Fig. 8. Block diagram of Impact Compensation using the CoP (IC^2).

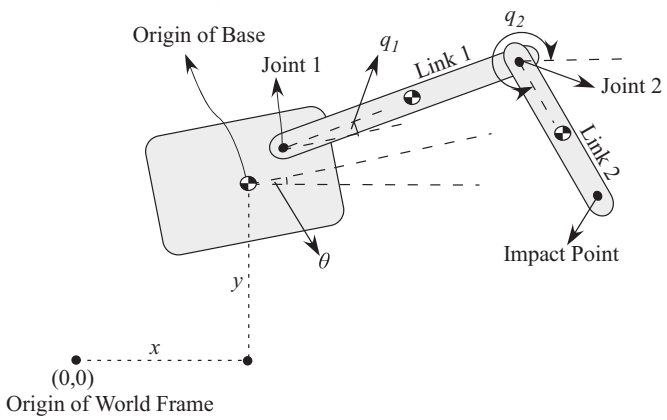

Fig. 9. The planar space robot used in the simulations.

Table 1
Physical characteristics of planar system.

Link	Mass (kg)	Inertia (kg-m^2)	Joint length (m)	CM (m)	CoP (m)
Base	300	50	N/A	0	–
1	30	3.33	1	0.3	0.67
2	20	2.5	1	0.3	0.72

where an acceleration $\ddot{\mathbf{q}}^*$ is calculated by,

$$\ddot{\mathbf{q}}^* = \ddot{\mathbf{q}}_d + \mathbf{K}_d(\dot{\mathbf{q}}_d - \dot{\mathbf{q}}) + \mathbf{K}_p(\mathbf{q}_d - \mathbf{q}) \tag{56}$$

where $\mathbf{q}_d$, $\dot{\mathbf{q}}_d$, $\ddot{\mathbf{q}}_d$ are the desired position, velocity and acceleration of all degrees of freedom in vectorial form and $\mathbf{K}_d$, $\mathbf{K}_p$ are the gain matrices for derivative and proportional control. Therefore the necessary torques are given by

$$\boldsymbol{\tau} = \hat{\mathbf{M}}\,\ddot{\mathbf{q}}^* + \hat{\mathbf{V}}(\mathbf{q}, \dot{\mathbf{q}}) \tag{57}$$

where $\hat{\mathbf{M}}$, $\hat{\mathbf{V}}$ are estimates of the mass matrix and nonlinear velocity terms, respectively. The detailed procedure of model-based control can be found in the literature (Craig, 2004). Then, as the impact occurs, the motor torques are given by (54), with the help of (51)–(53).

After each impact, the systems under impact are separated. Then the chaser will reach again the target (due to the inertia of the masses and their initial relative velocity) due to the model-based controller (57), and another impact will occur. This can be repeated several times (Doh, Chung & Youm, 2000), until the impacts are below a threshold where another control scheme (e.g. Impedance Control) can be used effectively. The proposed IC^2 controller can be used for all these impacts in order to reduce their negative results: (i) reduce the impact reaction forces on the joints and (ii) reduce the tendency to separate the chaser from the target.

After each impact, the systems under impact are separated. Then the chaser will reach again the target (due to the inertia of the masses and their initial relative velocity) using (57) and another impact will occur. This can be repeated several times (Doh et al., 2000), until the impacts are below a threshold where another control scheme (e.g. Impedance Control) can be used effectively. The proposed IC^2 controller can be used for all these impacts in order to reduce their negative results: (i) reduce the impact reaction forces on the joints and (ii) reduce the tendency to separate the chaser from the target.

As the impact is a process with fast dynamics, it is necessary to have a high performance motor drive. For the same reason, it is important to keep the computational effort to a minimum. The proposed method requires few and fast calculations, thus it is computationally feasible. By design, values as lengths, masses and inertias are known; therefore for (51)–(53) to be implemented, joint encoders and a force sensor at the last link N to detect the impact are required.

A closing note related to the estimation of the IP location is considered necessary. For (51) and (52), ${}^i\mathbf{r}_i$ i.e. the distance of joint $\{i+1\}$ or of the IP from the CoP of link $\{i\}$, must be known. In practice one can establish two cases: (a) the IP is known a priori and (b) the IP is unknown.

In the first case, the IP is known by design, or by a priori planning; as a result the equations can be used with this known value and any discrepancies due to inaccurate IP estimation will be low – the accepted inaccuracies can be estimated following the procedure of Section 3. It is expected that for man-made systems, this is the usual case.

If the IP is unknown, a method to compute this point is needed. Many researchers are working in the field; some notable works can be found in the literature (Bai & Tsai, 2011; Chen & Yuan, 2010; Choi & Chang, 1994). As expected, even though these are fast and can be used in real time, they add a small delay in the calculations.

5. Implementation guidelines

In this work, manipulators with revolute joints were assumed as this is the most common type in space robotic applications. For such manipulators, a number of guidelines for applying the developed methodology are given next.

First the case of free joints, or joints disengaged from their actuators rendering them essentially free, is examined. The following guidelines apply:

a. An impact should occur as near as possible to the measured CoP and at normal angle with respect to longitudinal axis which is defined by the RA (2D Case) or RP (3D Case) to the IP (see Section 3). To this end, the robotic system must prepare itself for the impact. The equations which describe the use of CoP are summarised by (21), (32), (33) and (35).
b. The rotation of revolute joints should be such that the links will be normal to each other at the moment of the impact, see (11) and connected at their CoP, see (45) (assuming the latter property is achievable).
c. To filter an impact in 2D systems, two revolute joints are needed, while in the 3D case, three revolute joints are needed, each corresponding to each component of the impact force.
d. In the presence of uncertainties, the configuration with successive normal links and a normal impact angle gives the best results, because this configuration can gradually filter most components of the impact force residues.

For joints engaged with actuators, the following guidelines also should apply:

e. In case of an impact at a point different from the CoP, an additional torque, computed using (51)–(53), should be applied to all rotational joints including the base.
f. In conjunction with guideline (e), the controller should apply the necessary torque to cancel friction.

6. Simulation results

In this section, a number of interesting cases is studied by simulations. The results are based on the analysis presented. As the earlier analysis has shown, the most interesting effects apply at a

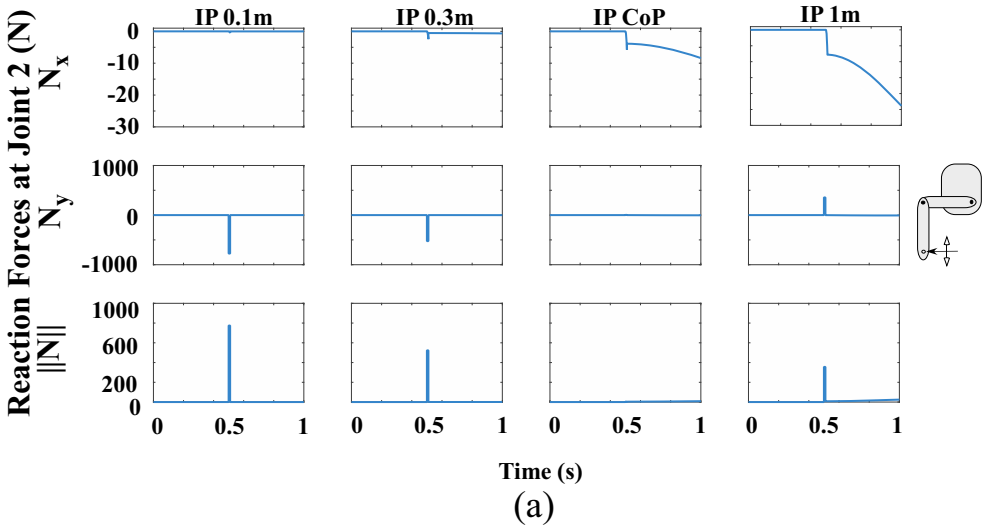

(a)

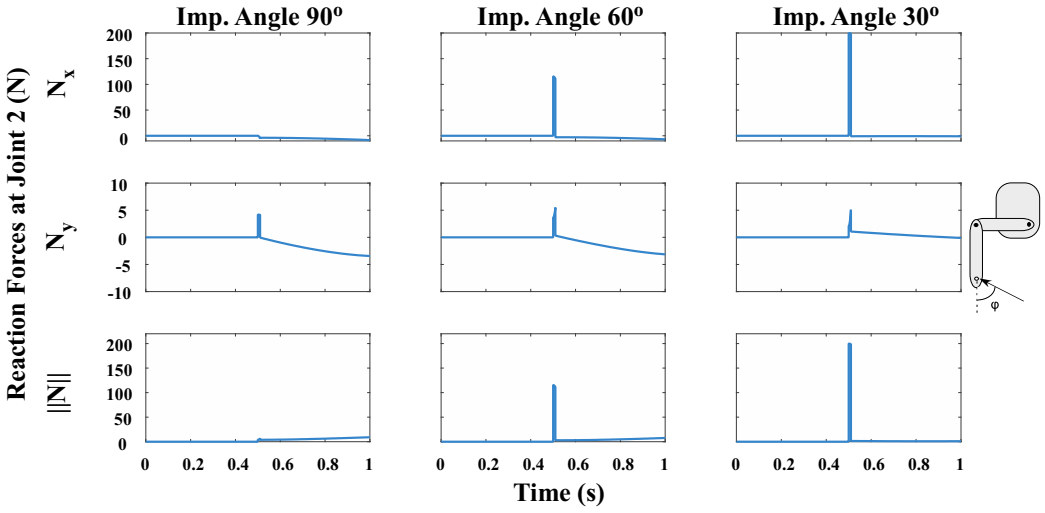

(b)

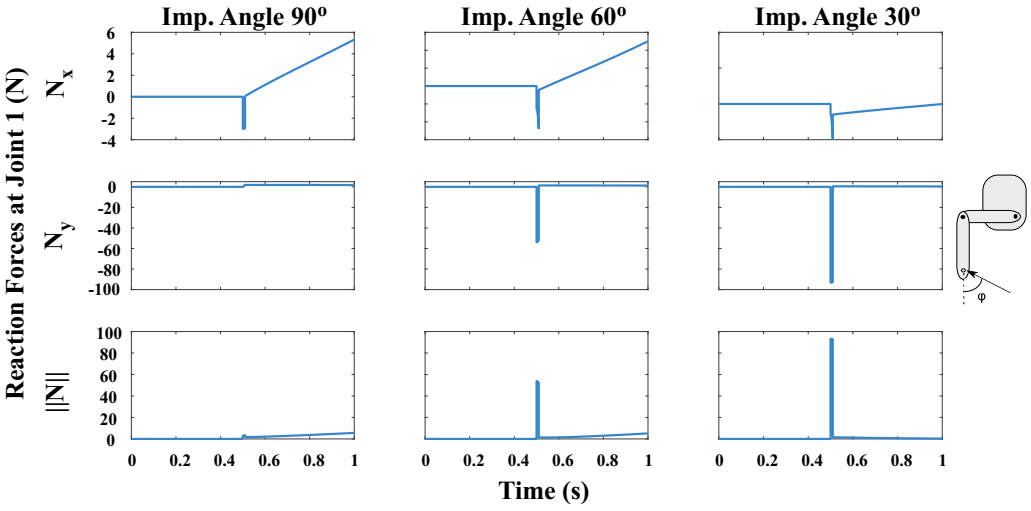

(c)

Fig. 10. Reaction forces on local coordinates after the impact on link 2: (a) at joint 2 with impact locations between 0.1 m and 1.0 m (b) at joint 2 with various angles of impact occurring at the CoP of link 2, and (c) at joint 1 for various impact angles while the position of joint 2 is at the CoP of link 1.

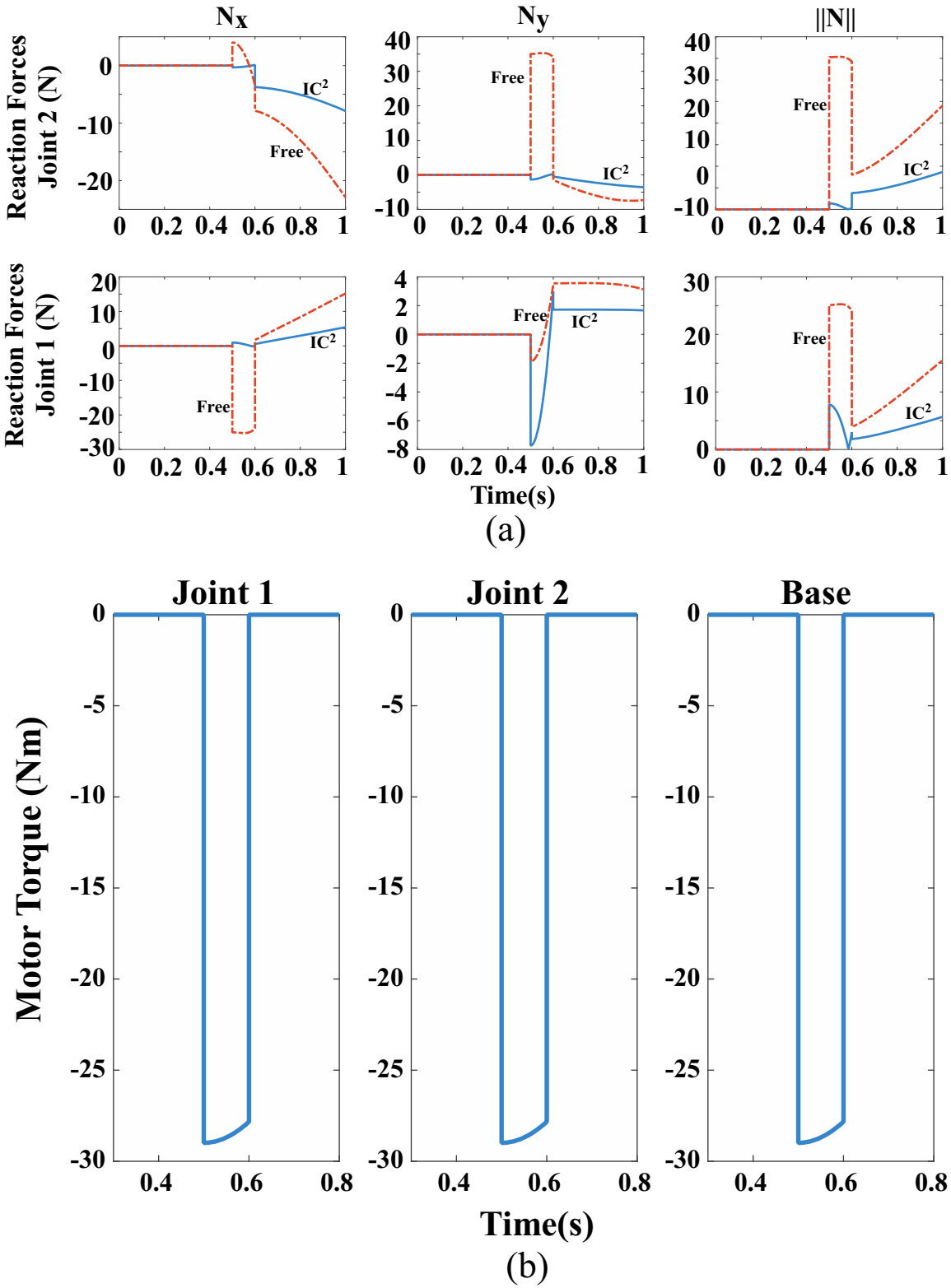

Fig. 11. Demonstration of the IC^2 controller: (a) Reaction forces at joints 1 and 2 when the robot has free joints or uses IC^2 and (b) Joint motor torques and base reaction wheel torque for the case the IC^2 is used.

specific plane. Therefore two general cases will be presented, i.e. a planar space robot with free joints, and the same with actuated joints. A 3D case is presented in a previous work (Paraskevas & Papadopoulos, 2013).

6.1. *Planar space robot with free joints*

The simulations refer to the planar system shown in Fig. 9, which consists of a thruster-equipped base, able to make *x*–*y*

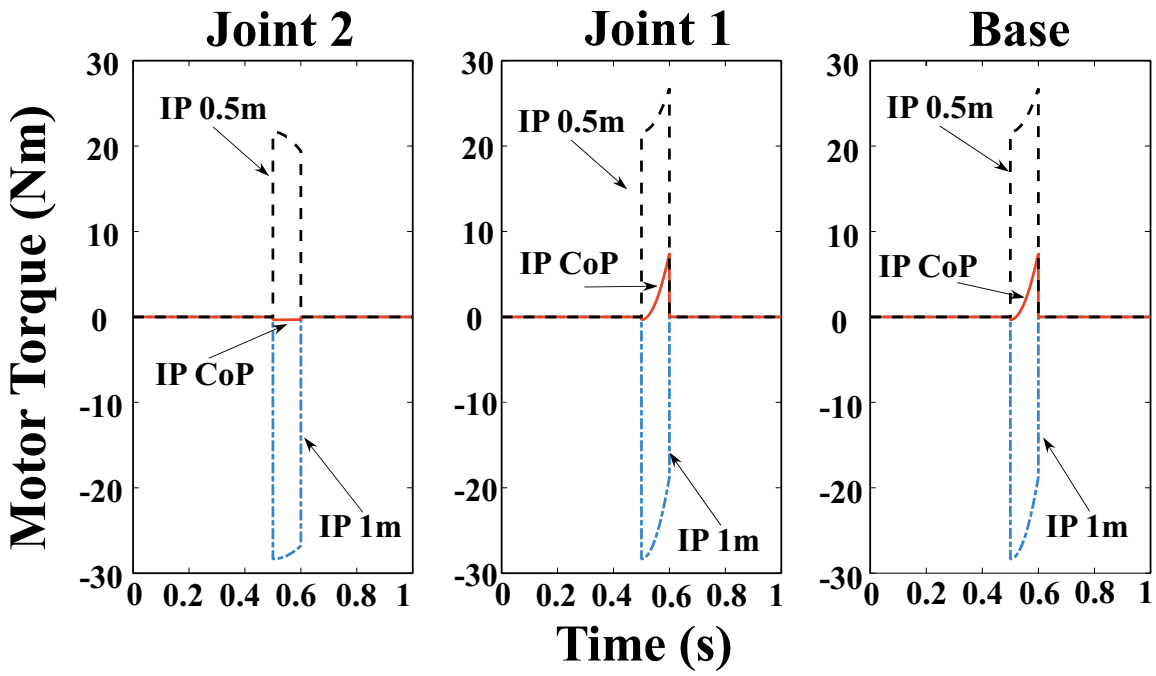

Fig. 12. Joint motor torques and base reaction wheel torque using IC^2 for various IP's.

translational planar and rotational motions, while the manipulator joints are free. Table 1 displays the physical properties of the system, including the position of CoP for the two rotational links. The first joint is located at (0.5 m, 0.5 m) from the centre of mass of the robot base. Note that this does not affect the CoP behaviour, only the motion of the base due to reaction forces.

Simulations were run by changing various parameters: (a) impact position on link 2, (b) impact angle, (c) position of joint 2 on link 1 and (d) initial angles of joints q_1 and q_2. The impact duration is 0.01 s, and the magnitude is set equal to 1 kN. To make the comparison of impact configurations easier, forces were plotted instead of impulses. Also, the plots present the force components on the local coordinate frame of each joint, i.e. the normal component of the impact force is parallel to the y_i axis of the local CS of link $\{i\}$.

Fig. 10 presents the reaction forces after the impact on link 2: (a) at joint 2 with impact locations between 0.1 m and 1.0 m (b) at joint 2 with various angles of impact occurring at the CoP of link 2, and (c) at joint 1 for various impact angles while the position of joint 2 is at the CoP of link 1 (which is always normal to link 2). As shown in Fig. 10a, the local reaction force is almost eliminated when the impact acts at the CoP, whereas in Fig. 10b, the reaction force is almost eliminated when the impact angle is normal to link 2. Note that after the impact the reaction forces may vary, however this is solely due to the post-impact free motion and the consequent dynamic coupling between the bodies. Similarly in Fig. 10c, the reaction force at joint 1 is almost zeroed when the impact angle is 90°.

These results validate the use of the CoP notion in minimizing the reaction impulses. More specifically it can be seen that when the impact occurs at the CoP at a normal angle, the reactions during the impact are minimized, thus the system has a smoother behaviour. When the impact does not occur at the CoP and/or with normal angle, there is always a residual reaction force propagating to the next link and eventually to the robot base.

6.2. *Planar space robot with actuated joints and IC^2*

To examine the performance of the IC^2 controller, a set of simulations was run based on the planar robot of Fig. 9. Here, the impact occurred at the end-effector at time $t=0.5$ s with duration 0.1 s and magnitude 100 N. For the application of IC^2, (51)–(53) were used, and the friction compensation was assumed to be ideal in order to examine the validity of the impact compensation part of the controller.

During simulations, the robot has two links in a normal configuration, i.e. $q_1 = -90°$ and $q_2 = 90°$. Joint 1 is located at the tip of link 1, thus further away from the CoP, and the impact occurs at various points of link 1, normal to the longitudinal axis of link 2, as the guidelines suggest. As it can be seen in Fig. 11, where the impact occurs at the tip of link 2, the use of the IC^2 reduces the reaction forces, without requiring large computational burden – this is critical as it can be applied within the duration of the impact. However it is important that the impact occurs at an ideal configuration, i.e. links normal to each other, impact angle normal to the link, impact point near the CoP, as it will reduce motor torque requirements considerably. Otherwise, large deviations will increase the force components that cannot be compensated for (i.e. components parallel to the link longitudinal axis), or the motor torques will reach saturation levels.

Finally Fig. 12 shows the required motor torques during impacts at different IPs. As the IP is further away from the CoP with respect to the CoM, the required torque direction is clockwise. As the IP is between the CoP and the CM, the torque changes sign, since it depends on the direction of the impact force. It is interesting to note that near the CoP, the torque is almost zero. It is not exactly zero, as the links start to rotate and thus a small torque is applied.

7. Conclusion

In this work the use of the CoP concept during impacts on space robots was presented. The theory of the CoP in 2D and 3D was discussed in a non-dimensional context. The Coefficient of Impact Design, which relates system parameters to the location of the impact point, was presented. This coefficient is useful when analysing the non-dimensional reaction impulse during an impact configuration. The effects of system parameters or impact configuration errors, on the reaction forces was studied. The analysis

concentrated on free rotating joints, however robotic joints are not necessarily disengaged from their actuation. To this end a control scheme was presented which compensates for the reaction forces developed due to impacts at points other than the CoP. Observing the proposed guidelines prior to and during the impact, the joint reaction forces can be minimized effectively. Simulations validated the developed analytical results.

Acknowledgements

This research has be co-financed by the European Union (European Social Fund-ESF) and Greek national funds through the Operational Program "Education and Lifelong Learning" of the National Strategic Reference Framework (NSRF)-Research Funding Program: Heracleitus II. Investing in knowledge society through the European Social Fund.

References

Alba, M., Prada, J. C. G., Meneses, J., & Rubio, H. (2010). *Mechanism and machine theory*, vol. 45. Elsevier pp. 1681–1693.

Arisumi, H., Chardonnet, J-R., Kheddar, A. & Yokoi, K. (2007). Dynamic lifting motion of humanoid robots. In *Proceedings of the international conference on robotics & automation* (pp. 2661–2667), Rome, Italy.

Åström, K. J., & Canudas-de-wit, C. (2008). Revisiting the LuGre friction model. *IEEE Control Systems Magazine* (pp. 101–114), 101–114.

Bai, Mingsian R., & Tsai, Yao Kun (2011). mpact localization combined with haptic feedback for touch panel applications based on the time-reversal approach. *The Journal of the Acoustical Society of America*, *129.3*, 1297–1305.

Chen, Chunlin, & Yuan, Fuh-Gwo (2010). Impact source identification in finite isotropic plates using a time-reversal method: theoretical study. *Smart Materials and Structures*, *19.10*, 105028.

Choi, Keeyoung, & Chang (1994). dentification of foreign object impact in structures using distributed sensors. *Journal of intelligent material systems and structures*, *5.6*, 864–869.

Craig, J. J. (2004). *Introduction to robotics: mechanics and control* (3rd ed.). Prentice Hall.

Cross, R. (2004). Centre of percussion of hand-held implements. *American Journal of Physics*, *72*(5), 622–630.

Dimitrov, D.N., & Yoshida, K. (2004). Momentum distribution in a space manipulator for facilitating the post-impact control. In *Proceedings of the international conference on intelligent robots and systems* (pp. 3345–3350). Sendai, Japan.

Doh, N., Chung, W.K., & Youm, Y. (2000). On hard contact force control, In *Proceedings of the IEEE/RSJ international conference on intelligent robots and systems (IROS)* (pp. 1528–1533). Takamatsu, Japan.

Fehse, W. (2008). *Automated rendezvous and docking of spacecraft*. Cambridge University Press.

Flores-Abad, A., Pham, K., & Ma, O. (2012). Control of a space robot for capturing a tumbling object. In *Proceedings of the international symposium on artificial intelligence, robotics and automation in space, i-SAIRAS*. Turin, Italy.

Hauschild, J.P. & Heppler, G.R. (2007). Control of harmonic drive motor actuated flexible linkages. In *Proceedings of the international conference on robotics & automation* (pp. 3451–3456) Rome, Italy.

Ioi, K., Kawabuchi, T., Suda, A. & Moriya, K. (2011). Mechanical and control design of caster for low vibrations and crashes of carts. In *Proceedings of the international conference on mechatronics and automation* (pp. 1688–1693). Beijing, China.

Kong, K., Moon, H., Hwang, B., Jeon, D., & Tomizuka, M. (2009). Impedance compensation of SUBAR for back-drivable force-mode actuation. *IEEE Transactions on Robotics*, *25*(3), 512–521.

Li, Z., & Mao, K. (2013). *Advances in Tribology*, *2013*.

Nef, T., & Lum, P. (2009). Improving backdrivability in geared rehabilitation robots. *Medical and Biological Engineering and Computing*, *4*(4), 441–447.

Papadopoulos, E. G., & Chasparis, G. C. (2004). Analysis and model-based control of servomechanisms with friction. *Journal of Dynamic Systems, Measurement, and Control*, *126*(4), 911–915.

Papadopoulos, E.G., & Moosavian, S.A.A. (1994). Dynamics & control of multi-arm space robots during chase & capture operations. In *Proceedings of the international conference on intelligent robots and systems* (pp. 1554–1561). Munich, Germany.

Papadopoulos, E.G. & Paraskevas, I.S. (2005). Design and configuration control of space robots undergoing impact. In *Proceedings of the 6th international ESA conference on GNC*. Loutraki, Greece.

Paraskevas, I.S. & Papadopoulos, E.G. (2013). On the use of the centre of percussion for space manipulators during impacts. In *Proceedings of the international conference on robotics & automation* (pp. 3469–3474). Karlsruhe, Germany.

Stronge, W. J. (2000). *Impact mechanics*. Cambridge University Press.

Svinin, M., Kaneko, M. & Yamamoto, M. (2011). On the percussion centre of flexible links. In *Proceedings of the IEEE international conference on robotics and automation* (ICRA) (pp. 330–335). Shangai, China.

Yoshida, K., & Nakanishi, H. (2003). Impedance matching in capturing a satellite by a space robot. In *Proceedings of the international conference on intelligent robots and systems* (pp. 3059–3064). Las Vegas, Nevada.

Yoshida, K., & Sashida, N. (1993). Modeling of impact dynamics and impulse minimization for space robots. In *Proceedings of the international conference on intelligent robots and systems* (pp. 2064–2069). Yokohama, Japan.